Autonomous Decentralized System Identification by Markov Parameter Estimation Using Distributed Smart Wireless Sensor Networks

Junhee Kim[1] and Jerome P. Lynch, M.ASCE[2]

Abstract: Decentralized data processing has the benefit of improving wireless monitoring system scalability, reducing the amount of wireless communications, and reducing overall power consumption. In this study, a system identification strategy for single-input multi-output (SIMO) subspace system identification is proposed based on Markov parameters. The method is specifically customized for embedment within the decentralized computational framework of a wireless sensor network. By using the computational resources of wireless sensors, individual sensor nodes perform local data processing to identify the Markov parameters of a structural system. The data storage and wireless communication requirements of Markov parameters are significantly less than that required by the original raw data, resulting in the preservation of scarce system resources such as communication bandwidth and battery power. Then, the estimated Markov parameters are wirelessly communicated to a wireless sensor network base station where the global structural properties are assembled by execution of the eigensystem realization algorithm, an indirect subspace system identification method. The proposed strategy is evaluated using input-output and output-only data recorded during dynamic testing of a cantilevered balcony in a historic building (Hill Auditorium, Ann Arbor, MI). **DOI: 10.1061/(ASCE)EM.1943-7889.0000359.**

CE Database subject headings: Parameters; Markov process; Identification; Probe instruments; Structural dynamics.

Author keywords: Markov parameters; Subspace identification; Wireless sensor network; Smart structures; Structural dynamics.

Introduction

The field of system identification has produced a suite of powerful mathematical tools that can accurately model the dynamic behavior of a complex engineered structure (Ljung 1999). Identified models have historically served as the basis for predicting structural responses to future loads, designing feedback control systems (Juang 1994) and for estimating the health of a structure (Doebling et al. 1998). Modal analysis was one of the earliest forms of frequency-domain system identification with modal parameters (e.g., modal frequencies, modal damping ratios, and mode shapes) extracted from measured input-output measurements data (Ewins 2000). In the system theory community, two time-domain methods emerged: parameterization-based prediction-error methods for system identification (Ljung 1999) followed by powerful parameterization-free (i.e., data-driven) subspace system identification methods (Viberg 1995). Subspace system identification for the estimation of state-space models of dynamic systems has gained popularity within the engineering community since the 1990s. Subspace system identification seeks mathematical models that optimally fit the measurement data available, skipping the need for parameterization (i.e., a mapping between the mathematical model and physical parameters). Subspace system identification finds its origins in the seminal work of Ho and Kalman (Ho and Kalman 1966), which provided a means of extracting a minimal realization of a state-space model based on impulse response functions. Later, stochastic realization (Akaike 1974) and data-driven subspace identification (Van Overschee and De Moor 1996) provided the community with additional mathematical tools for accurate state-space modeling of large, complex dynamic systems. Today, a number of subspace-based state-space system identification (4SID) techniques have been successfully applied for system identification of civil and mechanical dynamic systems, including reference-based stochastic subspace identification (SSI) (Peeters and Roeck 1999) and the eigensystem realization algorithm (ERA) (Juang and Pappa 1985).

Regardless of the system identification technique adopted, the underlying requirement of all system identification methods is the availability of data (i.e., measurement of the system input and output). To collect this data, data acquisition systems are necessary. The vast majority of systems used in the laboratory and field are wired-based systems with centralized architectures. Specifically, sensors installed in the system utilize wires to communicate measurements to the central data server where data are time-synchronized, digitized, and stored for off-line analysis. In some instances, automated data processing occurs in the data server (i.e., online analysis). Although wires provide a reliable conduit for the communication of measurement data, the extensive cabling requirements of permanent data acquisition systems in large civil structures detracts from their attractiveness. To overcome these limitations, wireless sensors have been proposed for structural monitoring (Straser and Kiremidjian 1998; Lynch et al. 2006). In addition to simplifying the installation of sensors in large structural systems, wireless sensors also offer on-board computing

[1]Research Fellow, Dept. of Civil and Environmental Engineering, Univ. of Michigan, Ann Arbor, MI 48109. E-mail: junhkim@umich.edu

[2]Associate Professor, Dept. of Civil and Environmental Engineering, Dept. of Electrical Engineering and Computer Science, Univ. of Michigan, Ann Arbor, MI 48109 (corresponding author). E-mail: jerlynch@umich.edu

Note. This manuscript was submitted on October 28, 2010; approved on November 28, 2011; published online on December 1, 2011. Discussion period open until October 1, 2012; separate discussions must be submitted for individual papers. This paper is part of the ***Journal of Engineering Mechanics***, Vol. 138, No. 5, May 1, 2012. ©ASCE, ISSN 0733-9399/2012/5-478–490/$25.00.

resources that can be used to locally process measurement data (Lynch et al. 2003; Nagayama and Spencer 2007). On-board computing reduces the amount of data to be transmitted; hence, "smart" wireless sensor nodes can utilize the shared communication channel in a more effective manner. Wireless transceivers also consume more power than microprocessors. Therefore, processing data at the node can be more power-efficient than communicating raw data wirelessly (Lynch et al. 2004), an important consideration when powering nodes from battery or power harvesting sources.

The centralized wired monitoring system architecture is often defined by a small number of computing nodes (i.e., data servers) each endowed with large memory and computational throughput capacity. In stark contrast, the computing environment offered by wireless sensor networks is highly decentralized with a large number of lightweight computing nodes (i.e., small memory and computational throughput capacity). Lynch et al. (2006) first proposed the concept of decentralized computing for structural system identification. That study aimed to extract mode shapes from time-synchronized wireless sensor data by having nodes locally calculate Fourier output spectra followed by peak-picking (PP) to identify modal frequencies. Mode shapes were then extracted in the network by having the imaginary component of the Fourier spectra at modal frequencies wirelessly exchanged. Nagayama and Spencer (2007) explored the embedment of the output-only natural excitation technique (NExT) for identification of free decay responses using system output data from which state-space models were estimated by the ERA method executed on a centralized server. More recently, Sim et al. (2010) extended the work of Nagayama and Spencer (2007) by utilizing the random decrement technique (RDT) instead of NExT. Zimmerman et al. (2008) proposed the adoption of a parallel computing paradigm to embed the frequency-domain decomposition (FDD) method in a wireless sensor network for automated mode shape extraction.

In this study, a single-input multi-output (SIMO) subspace system identification strategy ideally suited for the decentralized computing architecture of a wireless monitoring system is proposed. The low-cost Narada wireless node (Swartz et al. 2005), a low-power node that is capable of sensing, actuating, computing, and wireless communication, is adopted as the primary building block of the wireless monitoring system. The complexity of the linear time-invariant SIMO problem will be handled by decomposing the system analysis into parallel single-input single-output (SISO) systems that can be embedded within the computational framework of the wireless sensor network. Specifically, μ-Markov parameter extraction is embedded in each wireless sensor to extract SISO system information in a compressed manner (namely, in a finite number of Markov parameters). After μ-Markov parameter extraction is completed, nodes then wirelessly transmit their results to a centralized server in which the global system characteristics of the SIMO system are identified using the ERA method. The proposed decentralized system identification method is experimentally verified using input-output and output-only measurements derived during forced vibration testing of a large cantilevered auditorium balcony. To validate the accuracy of the wireless monitoring system, the dynamic system properties (i.e., modal frequencies, modal damping, and mode shapes) autonomously extracted are compared with those derived from data-driven subspace system identification conducted off-line using the same measurement data.

Realization-Based Subspace System Identification

Subspace system identification of linear time-invariant (LTI) systems enjoys a long history dating back more than 40 years. Over that period, a large suite of mathematical tools has been developed for the identification of state-space models from input and output data of a dynamic system. The methods associated with subspace-based state-space system identification (4SID) are generally categorized into one of two groups: realization-based and direct subspace methods (Viberg 1995). Realization-based 4SID methods find their origins in the seminal work of Ho and Kalman (Ho and Kalman 1966) and offer a means of estimation of state-space models. At the core of the realization-based 4SID methods is the need for a reliable estimate of system impulse responses, often termed the system Markov parameters (MP). Because the methods require a priori system impulse response estimation, the realization-based 4SID methods are also referred to as indirect 4SID methods. More recently, direct subspace methods (Van Overschee and De Moor 1994, 1996; Verhaegen 1994) have emerged as the preferred subspace approach for system identification because of their improved performance over realization-based 4SID. Direct 4SID methods, also referred to as data-driven subspace identification (Peeters and Ventura 2003), further generalize the realization-based methods with the state-space representation of a system derived from the time-history data without requiring the estimation of impulse response functions. A summary of the subspace-based state-space system identification methods is presented in Fig. 1.

Although direct 4SID methods are more accurate in estimating state-space models, their computational requirements exceed the processing and memory resources available at a wireless sensor node. In contrast, Markov parameter estimation for realization-based 4SID methods is computationally less resource-intensive and naturally decomposes the SIMO system into SISO systems. Decomposition is an attractive approach in the wireless sensor domain because it allows the wireless sensor nodes to be parallelized for the simultaneous estimation of SISO impulse response functions using a locally collected system output corresponding to a known system input. Estimation of impulse response functions can be accomplished by one of three methods: NExT (James and Carne 1992), observer/Kalman filter identification (OKID) (Juang et al. 1991), and μ-Markov parameter identification (μ-MPID) (Van Pelt and Bernstein 1998). The NExT method has been used for impulse response extraction using wireless sensor networks engaged in output-only structural monitoring in the study by Nagayama and Spencer (2007).

In this study, a realization-based 4SID method is embedded in a wireless sensor network using μ-Markov parameters to extract system impulse response functions from input-output data sets. The μ-Markov parameters compress the original output time-history data into a small number of parameters that can be wirelessly communicated using significantly less energy and communication bandwidth than by transmitting the original measured time-histories. Unlike OKID that requires a model order to be established a priori, the μ-MPID approach does not. This renders the method ideal when implemented in an automated monitoring system. MP sequences collected from each wireless sensor can be aggregated at a single server in which the state-space realization of the SIMO system is formed using the eigensystem realization algorithm (ERA) (Juang and Pappa 1985).

μ-Markov Parameter Estimation Using Input-Output Data

The μ-Markov parameter estimation technique is a time-domain technique used for the extraction of system impulse response

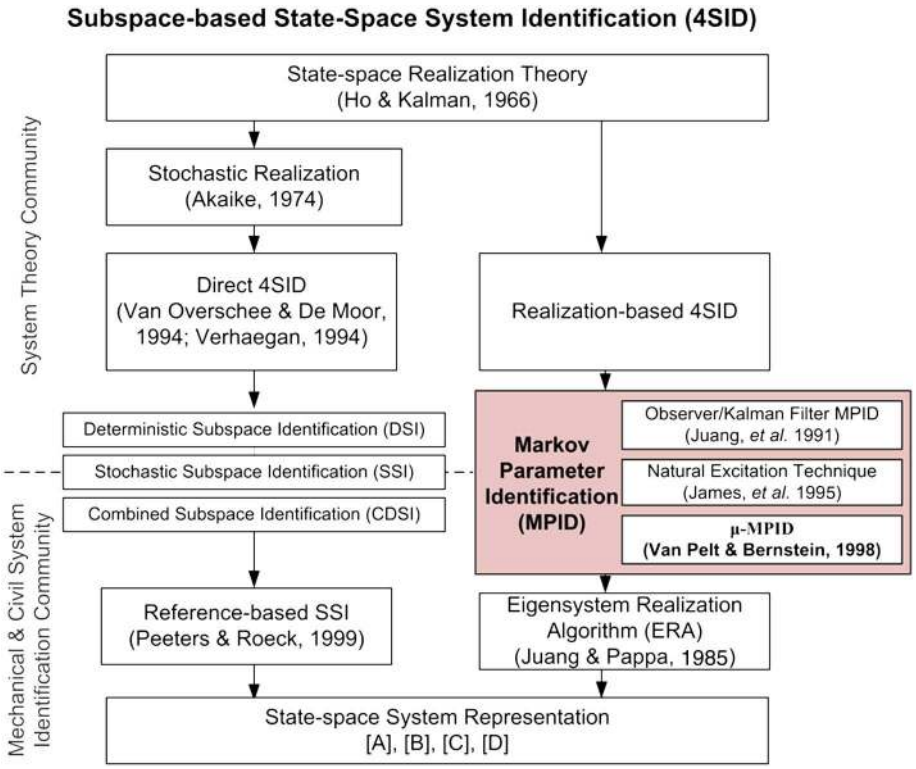

Fig. 1. Overview of the family of 4SID methods with the role of MP estimation highlighted

functions (Van Pelt and Bernstein 1998). Compared with more traditional time-domain techniques such as OKID (Juang et al. 1991), μ-Markov parameter estimation is conceptually simple and particularly well suited for embedment in fixed point microcontrollers commonly integrated with low-power wireless sensor nodes. Furthermore, it does not require a priori selection of the system model order to extract Markov parameters. This is in stark contrast to more traditional approaches to Markov parameter estimation such as the fitting of time-series models (e.g., AR, ARX, ARMA) and OKID.

Derivation of μ-Markov parameter estimation for a linear time-invariant SISO system begins with the nth order autoregressive moving average (ARMA) model:

$$y(k) = -\sum_{j=1}^{n} a_j y(k-j) + \sum_{j=0}^{n} b_j u(k-j) \tag{1}$$

where k = discrete time step; a_j = coefficients on the system output y; and b_j = coefficients on the system input u. If the at-rest system is excited by an impulse load at $k = 0$ [i.e., $u(0) = 1$ and $u(k) = 0$ when $k \neq 0$], then Eq. (1) at $k = 0$ simplifies to $y(0) = b_0$. Because the system output at $k = 0$ is the impulse response function, it can be extracted from the moving average (MA) part. Then, the ARMA model at step k to be rewritten

$$y(k) = -\sum_{j=1}^{n} a_j y(k-j) + h_0 u(0) + \sum_{j=1}^{n} b_j u(k-j) \tag{2}$$

By inserting the ARMA model at time $k-1$ into Eq. (2), another representation of the model can be derived as

$$y(k) = -\sum_{j=1}^{n} a'_j y(k-j-1) + \sum_{j=0}^{1} h_j u(k-j) + \sum_{j=1}^{n} b'_j u(k-j-1) \tag{3}$$

where a'_j and b'_j = modified system coefficients. Repeating this procedure $\mu - 1$ times, an ARMA equation explicitly displaying the first μ values of the impulse response function $(h_0, h_1, \ldots h_{\mu-1})$ is found:

$$y(k) = -\sum_{j=1}^{n} a_j^{(\mu-1)} y(k-j-\mu+1) + \sum_{j=0}^{\mu-1} h_j u(k-j) + \sum_{j=1}^{n} b_j^{(\mu-1)} u(k-j-\mu+1) \tag{4}$$

where h_0, h_1,$\ldots h_{\mu-1}$ = μ-Markov parameters. The ARMA model written in Eq. (4) has $2n + \mu$ unknowns: $a_j^{(\mu-1)}$, $b_j^{(\mu-1)}$, and h_j. A least-squares problem can be formulated to determine the unknowns using the measured input-output sequences of the LTI system.

Consider the system input and output of Eq. (4) assembled as a row vector, $\boldsymbol{\phi}_k$, at time step k:

$$\boldsymbol{\phi}_k = \{-y(k-\mu) \ \cdots \ -y(k-n-\mu+1) \ u(k) \ \cdots \ u(k-n-\mu+1)\} \in \Re^{1\times(2n+\mu)} \tag{5}$$

If the input-output response of the system is considered at each time step from $k = 0$ to $N-1$, then the input-output matrix can be formed:

$$\Phi = \left[\boldsymbol{\phi}_0^T \quad \boldsymbol{\phi}_1^T \quad \cdots \quad \boldsymbol{\phi}_{N-1}^T\right]^T \in \Re^{N\times(2n+\mu)} \tag{6}$$

The system output from $k = 0$ to $N - 1$ assembled as a column vector, $\mathbf{y} = [\, y(0) \quad \cdots \quad y(N-1)\,]^{\mathrm{T}}$, is linearly related to the unknown ARMA parameters

$$\boldsymbol{\theta} = [\, a_1^{(\mu-1)} \quad \cdots \quad a_n^{(\mu-1)} \quad h_0 \quad \cdots \quad h_{\mu-1} \quad b_1^{(\mu-1)} \quad \cdots \quad b_n^{(\mu-1)}\,]^{\mathrm{T}} \in \Re^{(2n+\mu)\times 1} \tag{7}$$

through the input-output matrix of Eq. (6):

$$\boldsymbol{y} = \Phi\boldsymbol{\theta} \tag{8}$$

If the number of observed points, N, is larger than the number of unknowns $(2n + \mu)$, Eq. (8) represents an overdetermined set of linear equations in which the unknown ARMA model parameters, $\boldsymbol{\theta}$, can be found by applying the traditional linear least-squares solution:

$$\boldsymbol{\theta} = (\Phi^T\Phi)^{-1}\Phi^T\boldsymbol{y} \tag{9}$$

The unknown ARMA parameter vector, $\boldsymbol{\theta}$, of Eq. (9) does not contain any parameterized information of the dynamic system; rather, the estimation of the finite impulse response function of the system is derived. This finite impulse response (FIR) model is in contrast to the infinite impulse response (IIR) model derived by classical parametric estimation methods.

The paramount benefit of μ-Markov parameter estimation compared with the direct application of conventional time-series models, is that the method extracts an accurate representation of the system impulse response function without requiring a priori selection of the system model order (e.g., selection of the number of weighted coefficients in the time-series model). Because system order is conventionally determined by manual methods, this step is difficult to reliably implement in an automated system identification system. Furthermore, poor model order selection can adversely affect the quality of the Markov parameters and subsequently degrade the performance of the overall system identification strategy. In contrast, estimated impulse responses by the μ-Markov parameter estimation are consistent regardless of the system order (Van Pelt and Bernstein 1998). It should be noted that implementation of the ERA algorithm at the central server does still require a priori determination of model order (e.g., typically through the use of stabilization diagrams), but this fact is independent of the origin of the Markov parameters extracted. Regardless, complete automation of the Markov parameter estimation as proposed herein represents a significant advancement over comparable methods that require a priori model selection for the extraction of Markov parameters.

Markov Parameter Estimation Using Output-Only Data

Estimation of a system free decay response function from output-only data by the random decrement technique was proposed by Ibrahim (Ibrahim 1977). Shortly thereafter, a new version of the Ibrahim time-domain (ITD) technique was proposed based on the cross-correlation between multiple system outputs recorded at different periods in time to extract the modal characteristics of a dynamic system (Ibrahim and Pappa 1982). The modal characteristics of the system are used to calculate the impulse response function of the system. A more effective output-only system identification method termed NExT was proposed by James et al. (1995). Conceptually, this method is analogous to stochastic realization-based on canonical correlation analysis (Akaike 1974). The major difference is the use of cross-correlation between a reference output and other system outputs, resulting in improved system identification. In this study, the NExT method is adopted to extract Markov parameters of the dynamic system. However, to be consistent with the description of the μ-Markov parameter estimation method previously described for the input-output data sets, the NExT method is described using parametric autoregressive models to derive the Markov parameters using output-only measurements of a dynamic system.

First, consider the ARMA model of the system defined in Eq. (1) for a defined reference output, $y_{\mathrm{ref}}(k)$:

$$y_{\mathrm{ref}}(k) = -\sum_{j=1}^{n} a_j y_{\mathrm{ref}}(k-j) + \sum_{j=0}^{n} b_j u(k-j) \tag{10}$$

If the lefthand and righthand sides of Eq. (10) are multiplied by another system output, $y_i(k-\tau)$, shifted in discrete time by τ, then the expected value of Eq. (10) is

$$E[y_i(k-\tau)y_{\mathrm{ref}}(k)] = -\sum_{j=1}^{n} a_j E[y_i(k-\tau)y_{\mathrm{ref}}(k-j)] + \sum_{j=0}^{n} b_j E[y_i(k-\tau)u(k-j)] \tag{11}$$

The expected value of the product of two time signals time shifted by τ relative to one another is defined as the cross-correlation function

$$R_{y_i y_{\mathrm{ref}}}(\tau) = E[y_i(k-\tau)y_{\mathrm{ref}}(k)] \tag{12}$$

Eq. (12) is therefore rewritten in terms of cross-correlation:

$$R_{y_i y_{\mathrm{ref}}}(\tau) = -\sum_{j=1}^{n} a_j R_{y_i y_{\mathrm{ref}}}(\tau-j) + \sum_{j=0}^{n} b_j R_{y_i u}(\tau-j) \tag{13}$$

The cross-correlation function between a system output and input is directly related to the autocorrelation of the system input through convolution:

$$R_{y_i u}(\tau-j) = h[-(\tau-j)] * R_{\mathrm{uu}}(\tau-j) \tag{14}$$

where $h(t)$ = impulse response of the system. If the input is assumed to be a stationary Gaussian random process, the autocorrelation function of the system input, R_{uu}, reduces to the Kronecker delta function, δ, scaled by an arbitrary constant, c_0' (James et al. 1995). This allows Eq. (13) to be rewritten

$$R_{y_i y_{\mathrm{ref}}}(\tau) = -\sum_{j=1}^{n} a_j R_{y_i y_{\mathrm{ref}}}(\tau-j) + c_0' h(0)\delta(\tau-j) \tag{15}$$

Hence, the cross-correlation between the system outputs is an infinite impulse response function with an identical AR model as that of the original system in Eq. (1).

Eigensystem Realization Algorithm

The eigensystem realization algorithm (ERA) (Juang and Pappa 1985) derives a minimal state-space realization of a linear time-invariant system using a finite number of Markov parameters as its input. ERA is therefore used in this study to derive the state-space model of a global SIMO system using the MP sequences of the SISO models previously derived from input-output and output-only measurements. The state-space representation of a fully controllable and observable system in the discrete time-domain is described as

$$\mathbf{x}(k+1) = \mathbf{A}\mathbf{x}(k) + \mathbf{B}u(k) \qquad \mathbf{y}(k) = \mathbf{C}\mathbf{x}(k) + \mathbf{D}u(k) \tag{16}$$

where $\mathbf{x}$ = n-dimensional state vector; $\mathbf{A} \in \Re^{n\times n}$ = system matrix; $\mathbf{B} \in \Re^{n\times 1}$ = vector relating the state to the single-input u; $\mathbf{C} \in \Re^{l\times n}$ = matrix relating the system observation vector, $\mathbf{y}$, to the state; and $\mathbf{D} \in \Re^{l\times 1}$ = vector relating the l system outputs to the single-input, u.

The controllability and observability matrices ($\mathcal{C}$ and $\mathcal{O}$, respectively) are defined as

$$\mathcal{C} = [\mathbf{B} \quad \mathbf{AB} \quad \cdots \quad \mathbf{A}^{n-1}\mathbf{B}] \tag{17}$$

$$\mathcal{O} = \begin{bmatrix} \mathbf{C} \\ \mathbf{CA} \\ \vdots \\ \mathbf{CA}^{n-1} \end{bmatrix} \tag{18}$$

The SIMO system is fully controllable and observable if, and only if, $\mathcal{C}$ and $\mathcal{O}$ are of rank n. If an LTI system is fully controllable and observable, then the vector of Markov parameters, $\mathbf{h}(k) = \{h_1(k)h_2(k)\ldots h_l(k)\}^T$, can be written as

$$\mathbf{h}(k) = \begin{cases} 0 & k < 0 \\ \mathbf{D} & k = 0 \\ \mathbf{CA^{k-1}B} & k > 0 \end{cases} \tag{19}$$

If an infinite sequence of MP are written in block Hankel form:

$$\mathcal{H} = \begin{bmatrix} \mathbf{h}(1) & \mathbf{h}(2) & \mathbf{h}(3) & \cdots \\ \mathbf{h}(2) & \mathbf{h}(3) & \mathbf{h}(4) & \cdots \\ \mathbf{h}(3) & \mathbf{h}(4) & \mathbf{h}(5) & \cdots \\ \vdots & \vdots & \vdots & \ddots \end{bmatrix} \tag{20}$$

then Eq. (19) allows the Hankel matrix to be factorized into an infinite observability and controllability matrix

$$\mathcal{H} = \begin{bmatrix} \mathbf{C} \\ \mathbf{CA} \\ \mathbf{CA}^2 \\ \vdots \end{bmatrix} [\mathbf{B} \quad \mathbf{AB} \quad \mathbf{A}^2\mathbf{B} \quad \cdots] = \mathcal{OC} \tag{21}$$

This allows the system matrices **A**, **B**, and **C** to be found by factorization of the Hankel matrix. If the rank of the block Hankel matrix is identical to the dimension of the system n, then the system matrices **A**, **B**, and **C** represent the minimal realization of the system. To achieve a minimal realization, the finite Hankel matrix can be robustly truncated to rank n through the use of singular value decomposition (SVD) (Kung 1978).

Implementation of MP System Identification within a Wireless Sensor Network

Input-output and output-only system identification based on Markov parameter extraction is ideally suited for implementation within the distributed computational architecture posed by a wireless structural monitoring system. Sensor-level computing is sufficient for the extraction of MPs from raw measurement data recorded by each wireless sensor node. After all sensor nodes have performed their MP extractions in parallel, the MPs from each node can be wirelessly communicated to the remaining nodes. Once Markov parameters have been collected from all measured degrees freedom, the eigensystem realization algorithm can be implemented at the network-level to estimate the system matrices **A**, **B**, and **C**. In this study, system identification based on Markov parameter extraction is implemented within a wireless structural monitoring system using three functional components: control server, local coordinator, and wireless sensor nodes (see Fig. 2). The control server is a single unit (e.g., a data server or wireless sensor) responsible for initiating and coordinating the data collection, communication, and computing tasks of the wireless monitoring system. The local coordinator is responsible for (1) applying a controlled excitation to the structure based on commands from the control server or (2) serving as a reference node during output-only analyses. The wireless sensor nodes are used to collect the acceleration response of a structure at their respective locations. In addition, wireless sensor nodes perform sensor-level computing when commanded by the local coordinator or control server. In this study, the Narada wireless sensor platform will serve as the system wireless sensor node and local coordinator; a standard personal computer (PC) will serve as the control server.

Narada-Based Wireless Structural Monitoring System

A low-cost wireless sensor previously proposed for monitoring civil structures is adopted. The wireless sensor platform (Fig. 3), termed Narada, was first proposed by Swartz et al. (2005) and has been successfully deployed in a number of full-scale structures for structural monitoring, including bridges (Kim et al. 2010), wind turbines (Swartz et al. 2010a), buildings, and naval ships (Swartz et al. 2010b). As a data acquisition platform, each Narada is capable of collecting data from transducers interfaced to its four sensing channels as long as sensor outputs are between 0 and 5 V. Each sensing channel is capable of digitizing data at a 16-bit resolution, with sampling rates as high as 100 kHz. In addition to a sensing interface, Narada also enjoys a two-channel actuation interface that can command actuators through a 0 to 4 V zero-order hold voltage signal. In this study, the actuation interface is exploited by the wireless monitoring system to apply a controlled excitation to a structure using an external actuator (e.g., electrodynamic shaker). Once data are collected, Narada employs a power-amplified IEEE 802.15.4 wireless transceiver (Chipcon CC2420) that can communicate to ranges well in excess of 100 m (line-of-sight) with over-the-air data rates of 250 kbp (Kim et al. 2010).

Most relevant to this study is the microcontroller core; this core allows Narada to process its measurement data locally. The computational core consists of an Atmel ATmega128 microcontroller operating at 8 MHz and featuring 128 kB of read only flash memory for the storage of embedded software. An additional 128 kB of random access memory (RAM) is incorporated to the Narada circuit to provide the microcontroller additional data storage capabilities. An operating system is written to the microcontroller flash memory for the automation of the node operation. The embedded operating system also allows the wireless sensor to be programmed with data processing algorithms that interrogate measurement data (Zimmerman et al. 2008; Zimmerman and Lynch 2009). Although Narada will be utilized in this study, it should be noted that any wireless sensor platform with on-board data processing capabilities (e.g., MEMSIC iMote2) can be used without modification to the proposed computational approach.

Input-Output Implementation

In the input-output implementation of the proposed automated system identification method [Fig. 2(a)], the control server coordinates the activities of the wireless monitoring system. The control server begins by broadcasting a command packet to the wireless sensor network notifying the local coordinator and the wireless sensor nodes that a test will begin. Upon receipt of that command packet, the coordinator and the wireless sensor nodes each acknowledge the receipt of the command and wait for time synchronization to occur. The control server then sends a beacon packet upon which

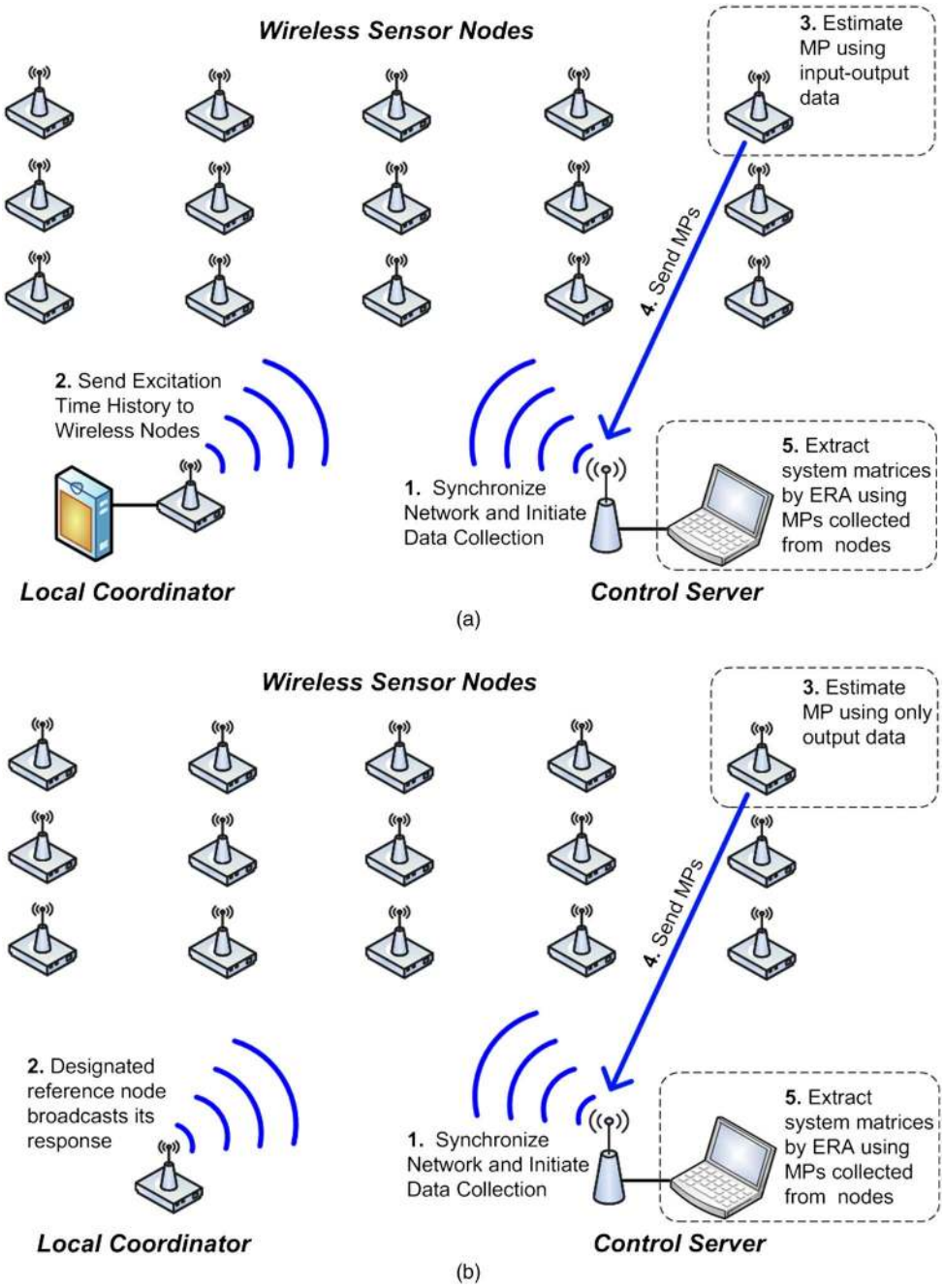

Fig. 2. Automated system identification by decentralized MP estimation within a wireless structural monitoring system: (a) input-output and (b) output-only implementations

the local coordinator and wireless sensor nodes initiate their internal clocks and begin their data collection tasks. This beacon-based approach to time-synchronization has been experimentally determined to be accurate with synchronization errors of less than 30 μs (Swartz et al. 2010a).

Upon receipt of the beacon packet from the control server, the local coordinator will begin the application of a controlled excitation to the structure (e.g., using a shaker) while the wireless sensor nodes record the structure response. After a number of time steps (N_{acc}) have been collected as defined by the control server during initiation of the network, the local coordinator stops its application of the excitation while the wireless sensor nodes simultaneously stop collecting structural response data. Next, the local coordinator broadcasts its raw excitation time-history record (i.e., in 16 bit integer format) to the network of wireless sensor nodes using a send-acknowledge communication protocol that ensures each wireless sensor node receives the excitation time-history record. Upon receipt of the excitation time-history record, each wireless sensor node converts the raw (16 bit) excitation, u, and acceleration time histories, y_i, into single-precision floating-point representations (32 bit). Next, each wireless sensor node extracts MPs using LU decomposition to solve Eq. (9). In total, N_{MP} parameters are estimated by each wireless sensor node.

After the sensor-level computing has been completed, each wireless sensor node confirms the completion of its computational task with the local coordinator. The local coordinator then requests each wireless sensor node to send its single-precision floating-point MP one at a time by peer-to-peer communication to the control

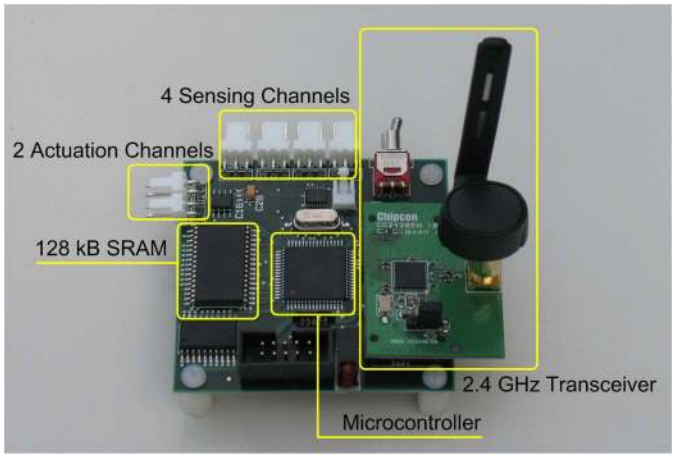

Fig. 3. Narada wireless sensing platform with key hardware components highlighted

server. Upon receipt of all MPs, the control server then assembles the MPs into an N_{MP} by N_{MP} Hankel matrix [Eq. (20)]. Singular value decomposition (SVD) of the Hankel matrix is performed by the central server; the SVD orthogonal matrices are truncated to rank n from which the system matrices **A**, **B**, and **C** are calculated.

The attraction of embedded μ-MP estimation is that sensor-level computing (i.e., MP estimation) results in a substantial compression of the measurement data prior to communication. This compression has two benefits: it preserves wireless bandwidth and can reduce the overall power consumption of the wireless sensor network. Consider a wireless monitoring system employing 15 Narada wireless sensor nodes ($N_{sensors}$) each collecting 1,200 time samples (N_{acc}) of measurement data at any arbitrary sample rate (f). If implemented in a centralized monitoring system, all of the wireless sensor nodes and the local coordinator would be required to communicate their raw (16 bit) time-history data to the centralized control server where system identification would be conducted. This would result in 38,400 bytes of data to be communicated (see Table 1). In the decentralized approach advocated herein, the local coordinator broadcasts its excitation time-history record (2,400 bytes) to the network so that each wireless sensor node can extract Markov parameters from their input-output data. Assuming 105 MPs are extracted with each parameter represented by a single-precision floating-point number (4 bytes), this generates 420 bytes worth of data to be communicated by each wireless sensor node. If all 15 wireless sensor nodes communicate their MPs to the control server, a total of 6,300 bytes would be communicated. Hence, the total number of bytes to be communicated by the decentralized μ-MP approach to system identification is 8,700 bytes (see Table 1). This represents a compression of more than 77%. If bandwidth is limited, this reduction in communicated data will alleviate demand for the wireless channel and hence, improve the overall scalability of the wireless sensor network (i.e., a greater number of nodes could be accommodated in the wireless sensor network). The amount of battery energy saved through compression is more difficult to analyze because such analyses are highly dependent on the wireless sensor hardware used and how that hardware is operated (i.e., whether portions of the hardware can be placed in low-power sleep or off states when not in use).

Table 1. Analysis of Communication Requirements of Centralized and Proposed Decentralized System Identification Methods

Methods	Transmission payload byte
Centralized implementation analysis performed on control server after all time-history records received	$N_{sensor} \times N_{acc} \times 2$ byte $=$ $16 \times 1{,}200 \times 2 = 38.4$ kbyte
Decentralized computing MP estimation conducted on wireless sensor nodes with MP communicated to control server	$N_{acc} \times 2$ byte $+ (N_{sensor} - 1) \times N_{MP} \times 4$ byte $= 1{,}200 \times 2 + 15 \times 105 \times 4 = 8.7$ kbyte
	$\therefore$ Transmission reduction $= \sim 77\%$

Note: network size, $N_{sensor} = 16$ units; time-history data length, $N_{acc} = 1{,}200$ points; number of Markov Parameters, $N_{MP} = 105$ points.

Output-Only Implementation

In the output-only implementation [Fig. 2(b)], the local coordinator is no longer responsible for the excitation of the structure but rather represents a reference node at which one additional channel of structural response is collected by the wireless monitoring system. Similar to the input-output implementation, the control server begins by synchronizing the network through the use of a beacon packet. Upon receipt of the beacon packet, the local coordinator and wireless sensor nodes reset their internal clocks and begin to collect structural response data for the prescribed time period. After N_{acc} time steps have been collected, the local coordinator broadcasts its raw (16 bits) time-history response, y_{ref}, to the wireless sensor nodes. By using Eq. (15), each wireless sensor node calculates the cross-correlation between its measured response, y_i, and that of the local coordinator's reference response, y_{ref}. Again, the calculation of the cross-correlation requires the sequential shifting of one output relative to another as a function of time offset, τ. The first 105 terms of the single-precision floating-point cross-correlation function, $R_{y_i y_{ref}}(\tau)$, are treated as MP to be communicated by each wireless sensor node to the control server for use in its ERA analysis. Because the communication requirements are identical to that of the input-output implementation, the amount of communication reduction (and corresponding savings in battery power) are the same as that presented in Table 1.

Experimental Validation—Vibration Testing of Hill Auditorium

Experimental validation of the proposed wireless monitoring system is conducted using a cantilevered balcony of Hill Auditorium, an historic theater on the University of Michigan's Ann Arbor campus. Constructed in 1913, the theater has a capacity of 3,500 seats with its seating distributed between the main floor and two balcony sections (termed the mezzanine and upper balconies). In this study, the mezzanine balcony was selected to serve as a demonstration structure for experimental validation of the decentralized system identification method embedded within a wireless monitoring system. The mezzanine balcony is roughly 42 m wide and is cantilevered 11 m above the main floor of the theater as shown in Fig. 4. The plan view presented in Fig. 5(a) reveals the supports of the balcony: rigid walls on two sides, a rigid wall on the back of the balcony, and six auxiliary columns distributed along the rear of the balcony.

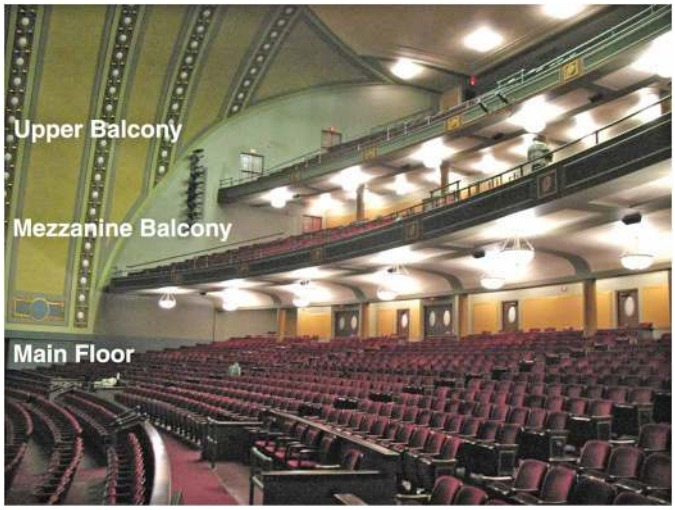

Fig. 4. Main floor, mezzanine, and upper balcony sections of the university of Michigan's Hill Auditorium (Ann Arbor, MI)

Instrumentation Strategy

A total of 15 Narada units is installed on the mezzanine balcony of Hill Auditorium; the wireless sensor nodes are organized into three rows of five nodes each as shown in Fig. 5(a). The wireless sensor nodes are number 1 through 15. Attached to each Narada node is an accelerometer mounted to the balcony floor to measure its vertical acceleration response. Two accelerometers are used: Crossbow CXL02 and PCB Piezotronics 3801D1FB3G. The sensitivity of the 3801D1FB3G accelerometer is 0.7 V/g, its acceleration range is ± 3 g, and its noise floor level is 0.15 mg. The CXL02 accelerometer sensitivity is 1 V/g, its range is ± 2 g, and its noise floor is 0.5 mg. To improve the signal-to-noise ratio of the accelerometers, a signal conditioning board designed to band-pass (0.014 to 25 Hz) and amplify (by 5, 10 or 20 times) sensor signals is utilized as shown in Fig. 5(d). In this study, an amplification of 20 is used on each accelerometer output before being digitized by the Narada analog-to-digital converter (ADC). The wireless sensor network is controlled by a standard laptop computer configured to act as the monitoring system's control server as shown in Fig. 5(b).

In the input-output implementation of system identification, an electrodynamic shaker (APS Dynamics 400) is used. The shaker [Fig. 5(c)] is placed at the front edge of the mezzanine balcony at the end of the third aisle [Fig. 5(a)]. This location is determined to be optimal for exciting a maximum number of modes of the cantilevered balcony. The shaker's total mass is 90.9 kg but its moving reaction mass is 20.7 kg. The shaker is controlled by a Narada node configured as a local coordinator [denoted as node 16 in Fig. 5(a)]. Prior to application of the Narada's digital-to-analog converter (DAC) output signal, the signal is boosted by an amplifier (Power Amplifier Model 124). The local coordinator is programmed to generate a saw-tooth chirp excitation with a frequency range of 3 to 15 Hz. To measure the motion of the shaker reaction mass, a Crossbow CXL02 accelerometer is mounted to the reaction mass

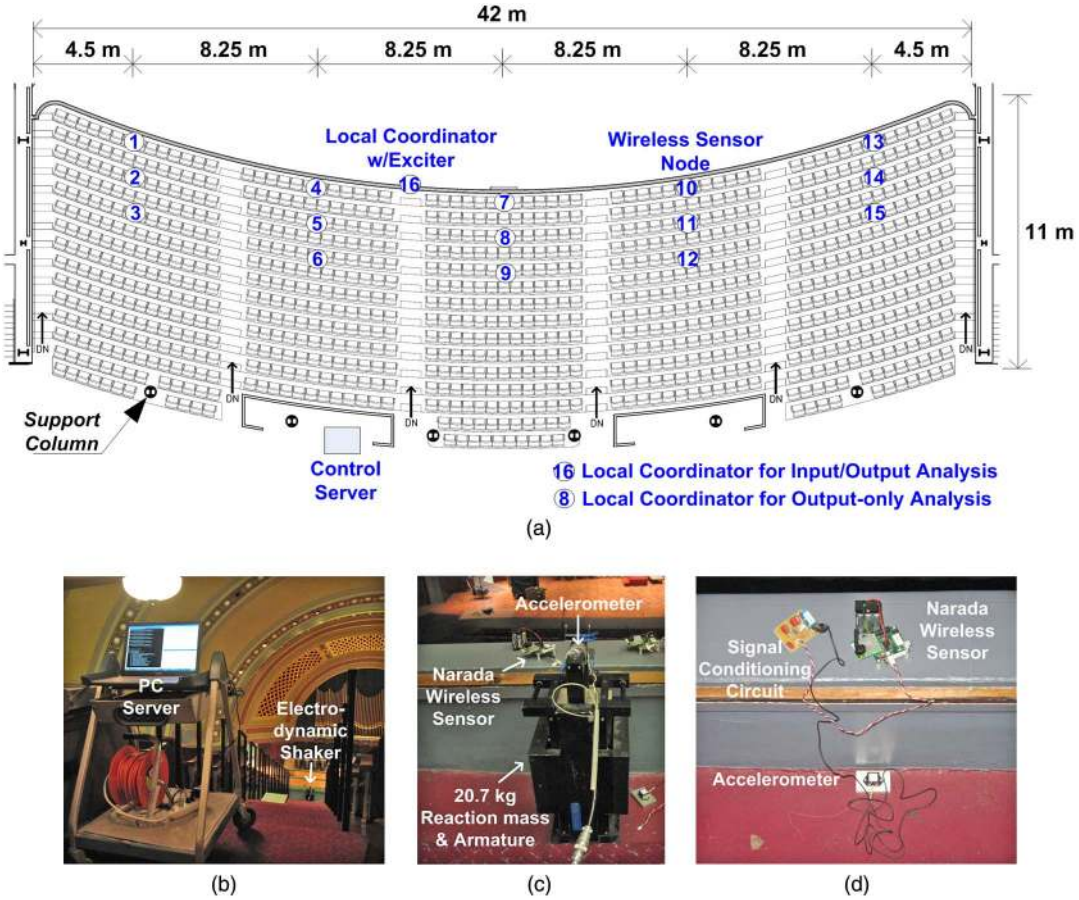

Fig. 5. Experimental setup of the wireless monitoring system on the mezzanine balcony of Hill Auditorium: (a) sensor and exciter locations; (b) the control server; (c) electrodynamic shaker driven by Narada; (d) typical Narada wireless sensor node with a MEMS-based accelerometer

and interfaced to the Narada node. During excitation of the balcony, five excitation types are utilized, with time of duration the primary differentiator between excitations. The durations of the chirp excitations are varied from 8 to 24 s in 4-s increments.

To validate the output-only system identification strategy, a broad-band white excitation source is utilized. Although the implementation of many output-only system identification methods record the behavior of the structure to ambient excitations (making the assumption that the ambient excitation is white and broad-band), this study utilizes impulsive loads as an equivalent broad-band excitation source. Toward this end, a soft-tip 5.44-kg (12-lb) modal hammer (Dytran Instruments 5803A) is used to introduce an impulse load in the vicinity of the electrodynamic shaker. Although a load cell is contained in the hammer tip, the measured force time history is not used during system identification. During the output-only implementation of the system, wireless sensor node 8 [Fig. 5(a)] is designated as the local coordinator of the wireless monitoring system. This selection is arbitrary with any other node capable of being the reference node; an investigation of different reference nodes reveals the results are relatively insensitive to which node serves as the reference.

With the first five modes estimated to be below 10 Hz, a sampling rate of 40 Hz is prescribed for all of the tests conducted in this study. Each test is conducted for 30 s, resulting in the collection of 1,200 points of data by the local coordinator and wireless sensor nodes. The input-output and output-only approaches to MP extraction are conducted autonomously by the wireless monitoring system. Each wireless sensor node is programmed to extract 105 Markov parameters.

Experimental Results

The acceleration of the shaker reaction mass during the application of the 20-s chirp signal as measured by the local coordinator (Narada node 16) is presented in Fig. 6(a). Because of the presence of a back electromagnetic field (EMF), the amplitude of the acceleration decreases over the duration of the applied excitation. In addition, the coupling between the shaker and the balcony is evident in the measured acceleration toward the end of the time-history record (i.e., between 16 and 20 s). The Fourier spectrum of the reaction mass acceleration is presented in Fig. 6(b). The 3- to 15-Hz frequency band of the applied excitation is confirmed, although the spectrum amplitude decreases at higher frequencies as a result of the aforementioned back EMF effect inherent to the excitation source. The acceleration response of the mezzanine balcony at the center of the balcony as measured by wireless sensor nodes 7, 8, and 9 is shown in Fig. 7. The acceleration response is less than 3 mg as measured in the three locations. In addition, resonance of the lower modes of the mezzanine balcony is evident in the first 10 s of the measured acceleration response. The power spectral density (PSD) functions corresponding to the response time histories plotted in Fig. 7 are shown in Fig. 8; the modes of the system are easy to identify in the PSD plots.

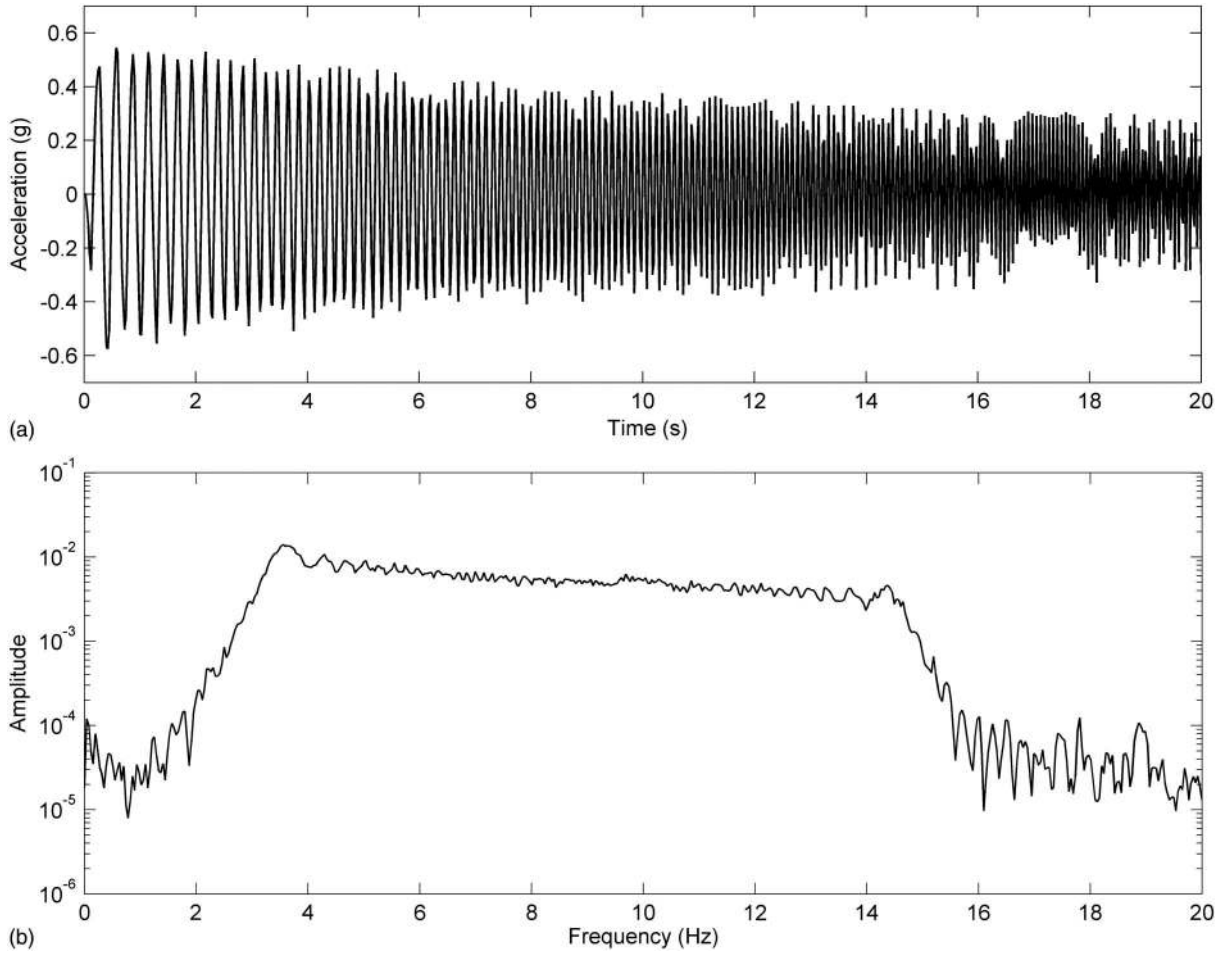

Fig. 6. Controlled excitation of the mezzanine balcony: (a) measured acceleration of the electrodynamic shaker reaction mass; (b) corresponding Fourier spectrum of the excitation

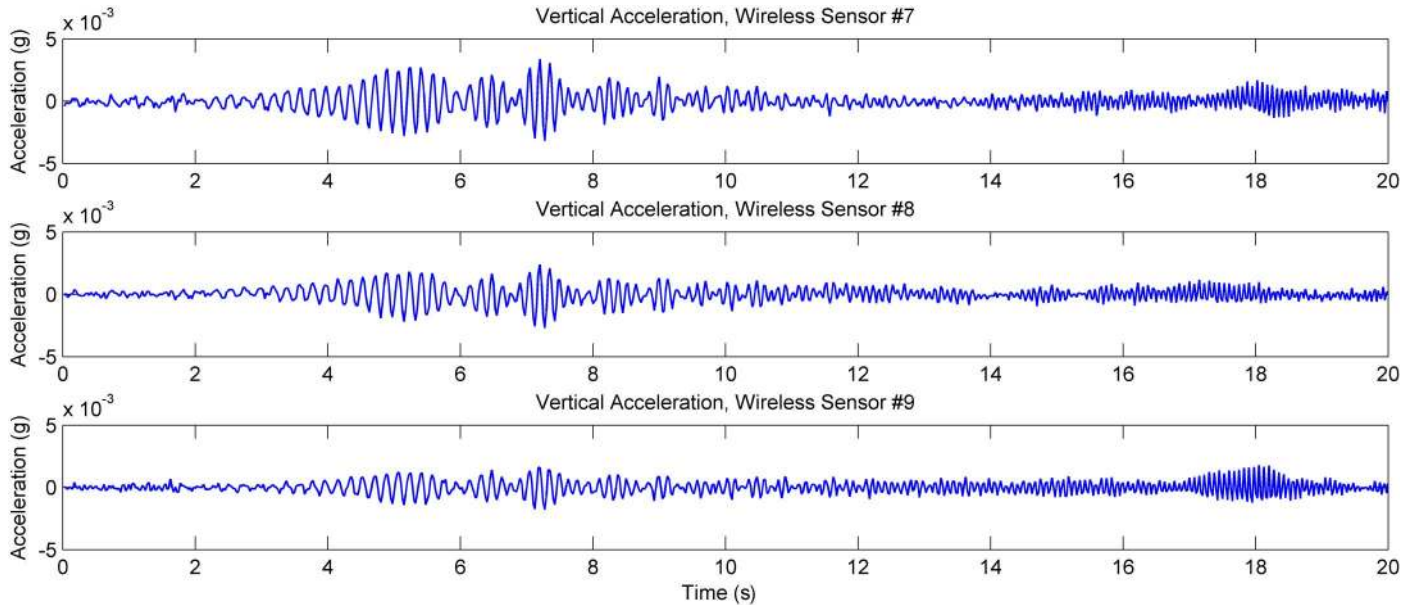

Fig. 7. Measured acceleration response of the instrumented mezzanine balcony at node 7 (top), 8 (middle), and 9 (bottom) during the application of a 20-s 3- to 15-Hz chirp signal (Fig. 6)

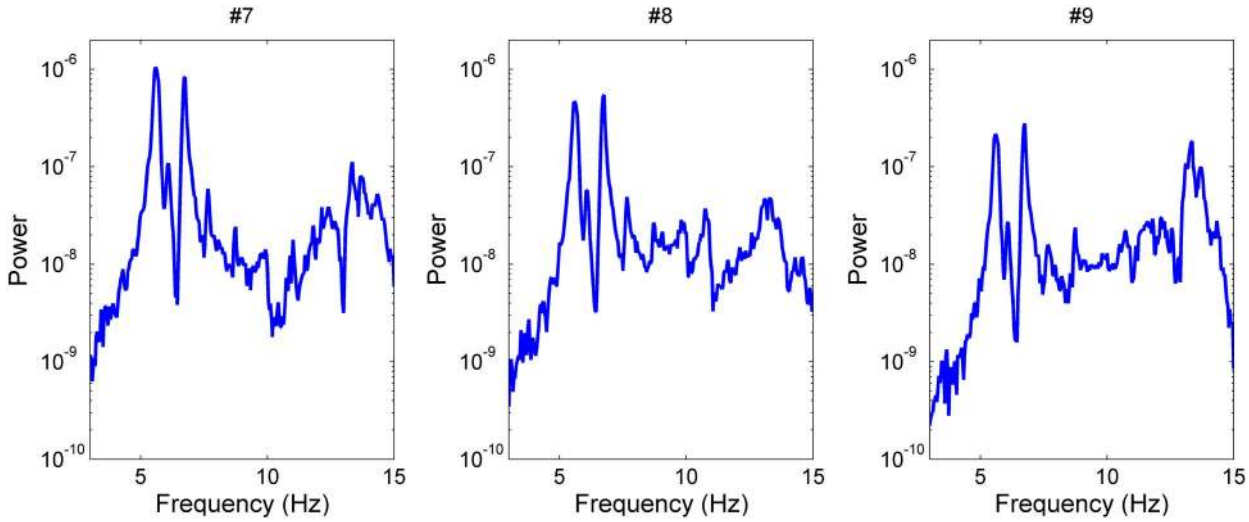

Fig. 8. Power spectral density functions of the measured acceleration response at sensor node 7 (left), 8 (middle), and 9 (right) during the application of a 20-s 3- to 15-Hz chirp signal (Fig. 6)

The wireless monitoring system automatically extracts the MPs at each wireless sensor node using the input-output or output-only data. During the input-output implementation of the decentralized system identification, perfect communication is experienced with data never lost during the broadcasting of the excitation force by the local coordinator and the communication of the MPs from each wireless sensor node to the control server. Similarly, the output-only implementation also experiences perfect communication with 100% data delivery during the broadcasting of the local coordinator acceleration response and the communication of the MPs from each wireless sensor node. Figs. 9 and 10 depict the estimated MPs as calculated by wireless sensor nodes 7, 8, and 9 during the input-output and output-only implementations, respectively. To check the precision of the extracted MPs, off-line subspace identification (i.e., direct 4SID in Fig. 1) is conducted using the excitation and response time-history data collected by the wireless monitoring system. Then, the MPs are simulated by applying an impulse input to the state-space model that was estimated using off-line subspace identification. As shown in Figs. 9 and 10, excellent agreement is encountered in the MP time histories. It should be noted that the decentralized MPs are calculated from individual parallel SISO systems by μ-MPID. In contrast, NExT and off-line MPs are calculated from the global SIMO system by the direct 4SID method. Thus, small discrepancies between the two results are found.

After the estimated MPs are communicated to the control server, the system matrices **A**, **B**, **C**, and **D** are estimated by ERA. The modal characteristics of the system (i.e., modal frequencies, mode shapes, and modal damping ratios) are extracted from the system matrix **A**. For example, the first five mode shapes of the mezzanine balcony as extracted by the input-output and output-only MP estimation are presented in Figs. 11(a) and 11(b), respectively. For comparison, the first five mode shapes of the balcony calculated off-line by subspace identification are also presented in Fig. 11(c).

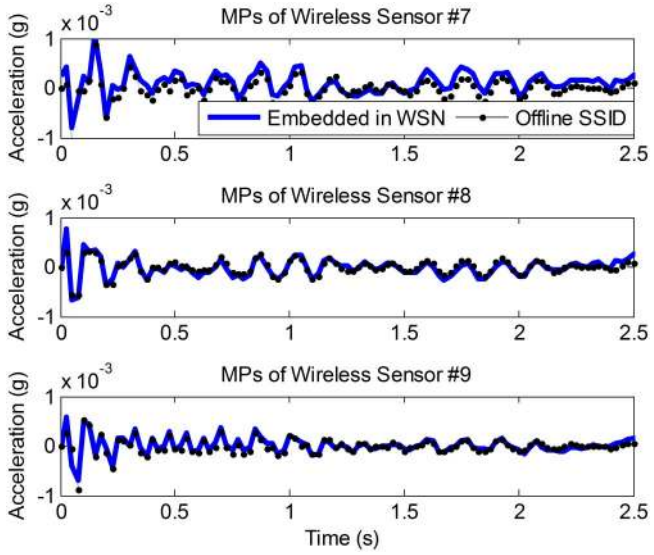

Fig. 9. Estimated MPs at wireless sensor node 7 (top), 8 (middle), and 9 (bottom) during controlled excitation of the balcony

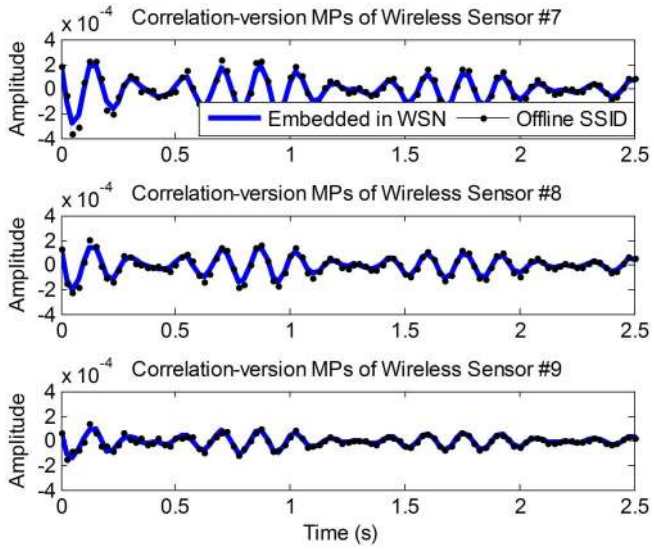

Fig. 10. Estimated MPs at wireless sensor node 7 (top), 8 (middle), and 9 (bottom) during output-only implementation of the decentralized system identification method

Strong agreement is visually observed in the mode shapes as estimated by the three independent system identification methods. To compare the modal characteristics extracted by the input-output and output-only implementations in a more quantitative manner, Table 2 tabulates the modal frequencies and modal damping ratios extracted by the three system identification methods (i.e., the in-network input-output implementation, in-network output-only implementation, and off-line subspace identification). During the input-output implementation, the five tests correspond to the same excitation but of differing duration (i.e., 8, 12, 16, 20, and 24 s). The five tests corresponding to the output-only implementation are separate modal hammer blows delivered to the balcony. The first four modal frequencies (5.6, 6.1, 6.7, and 7.6 Hz) and damping ratios (1.4, 1.1, 0.8, and 0.8 %) are all in strong agreement between the three system identification methods. However, the in-network implementation (both the input-ouput and output-only implementations) are not as accurate for the fifth mode (9.1 Hz). Compared with the off-line subspace identification method, the frequency and damping ratio of the fifth mode for the in-network input-output system identification method is in error by 5.5 and 81.6%, respectively. The modal frequency is more accurate for the output-only implementation (with an error of less than 1%); however, the estimated damping ratio is in error by 73.5%. To compare the mode shapes, the modal assurance criteria (MAC) is adopted (Ewins 2000). The mode shapes estimated by the wireless monitoring system are compared with the mode shapes extracted off-line. Again, consistent modes are extracted by the monitoring system as seen by MAC values close to 1 for the first four modes (which contain the majority of the response energy of the structure).

A power analysis is performed on the decentralized Markov parameter extraction process. The Narada wireless sensor has two major components that consume power: the wireless transceiver and microcontroller. The wireless transceiver (Chipcon CC2420) consumes approximately 59 mW (18 mA at 3.3 V) when transmitting or receiving. The radio can be placed into an idle state when not in use to preserve power; when idle, the transceiver consumes 1.4 mW (0.43 mA at 3.3 V). The microcontroller (Atmel ATmega128) consumes 85 mW of power (17 mA at 5 V and 8 MHz) but is constantly consuming power regardless whether it is computing. If no embedded computing is used (i.e., centralized implementation), then the 16 Narada nodes (inclusive of the reference node) each collects 1,200 time samples (40 Hz for 30 s) and communicates that to the central server (a total of 38,400 bytes transmitted). In this study's implementation, the radio is used to transmit data (raw time-history data and Markov parameters)

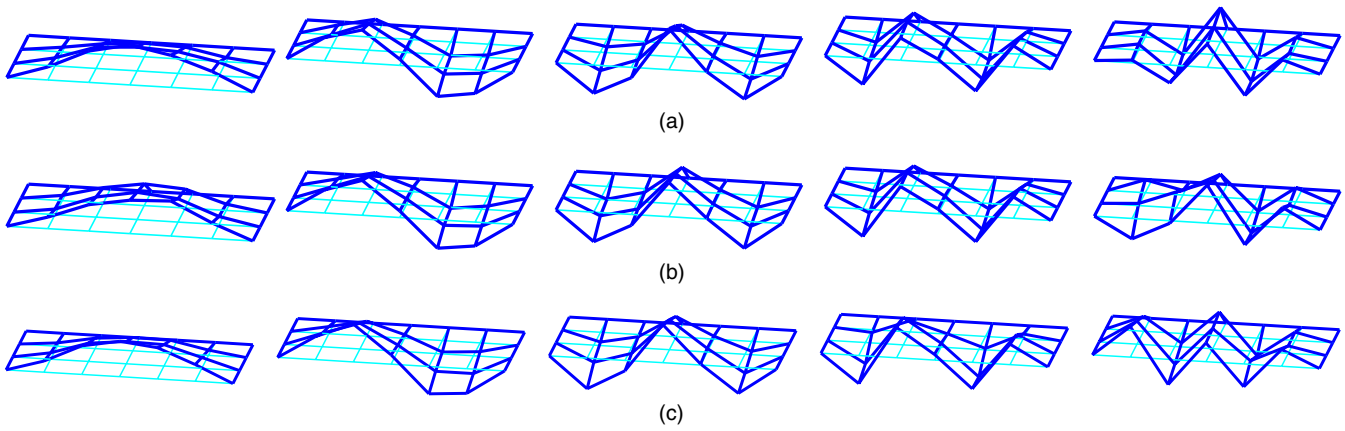

Fig. 11. Estimated five global mode shapes of the Hill Auditorium mezzanine balcony: (a) network-level ERA from sensor-level MP estimations from input/output data; (b) network-level ERA from sensor-level MP estimations from output-only data; (c) off-line subspace method from input/output data

Table 2. Summary of Identified Modal Parameters from the Hill Auditorium Mezzanine Balcony

	Input/output analysis					Output-only analysis				
Frequency (Hz)	Mode 1	Mode 2	Mode 3	Mode 4	Mode 5	Mode 1	Mode 2	Mode 3	Mode 4	Mode 5
Test 1	5.616	6.052	6.724	7.618	8.606	5.629	6.064	6.731	7.616	9.958
Test 2	5.629	6.046	6.720	7.613	8.591	5.617	6.030	6.727	7.638	8.535
Test 3	5.617	6.047	6.713	7.612	8.642	5.618	6.054	6.720	7.613	10.055
Test 4	5.612	6.047	6.717	7.610	8.663	5.611	6.045	6.718	7.620	8.660
Test 5	5.612	6.047	6.715	7.602	8.596	5.622	6.044	6.716	7.602	8.591
Mean	5.617	6.048	6.718	7.611	8.619	5.619	6.047	6.722	7.618	9.160
Subspace method	5.631	6.056	6.727	7.626	9.116					
Damping ratio	Mode 1	Mode 2	Mode 3	Mode 4	Mode 5	Mode 1	Mode 2	Mode 3	Mode 4	Mode 5
Test 1	0.014	0.011	0.007	0.008	0.011	0.011	0.008	0.007	0.007	0.022
Test 2	0.013	0.011	0.008	0.008	0.009	0.013	0.010	0.009	0.007	0.008
Test 3	0.013	0.012	0.008	0.008	0.005	0.014	0.011	0.007	0.007	0.014
Test 4	0.014	0.012	0.009	0.007	0.010	0.015	0.009	0.008	0.007	0.015
Test 5	0.013	0.012	0.009	0.008	0.008	0.015	0.011	0.008	0.006	0.007
Mean	0.013	0.011	0.008	0.008	0.009	0.013	0.010	0.008	0.007	0.013
Subspace method	0.014	0.011	0.008	0.008	0.049					
MAC	Mode 1	Mode 2	Mode 3	Mode 4	Mode 5	Mode 1	Mode 2	Mode 3	Mode 4	Mode 5
Test 1	0.998	0.969	0.999	0.933	0.480	0.977	0.994	0.992	0.972	0.543
Test 2	0.999	0.989	0.996	0.932	0.598	0.966	0.990	0.984	0.965	0.621
Test 3	0.999	0.983	0.996	0.935	0.495	0.972	0.996	0.994	0.973	0.474
Test 4	0.996	0.986	0.994	0.931	0.710	0.972	0.994	0.991	0.960	0.233
Test 5	0.999	0.982	0.992	0.933	0.455	0.975	0.992	0.990	0.969	0.524
Mean	0.998	0.982	0.995	0.933	0.548	0.973	0.993	0.990	0.968	0.479

and then placed in an idle state after all network transmissions have been completed. More specific, the radios are kept in active state even when not transmitting and only go to idle when all of the wireless sensors have completed their transfer of data. This is necessary to ensure all nodes can be commanded by the central coordinator. Assuming an effective bandwidth of 150 kbp, all of the transceivers must remain active for 2.05 s, and therefore each consumes 121 mJ. In the decentralized MP extraction process (both input-output and output-only), 15 Narada nodes receive 1,200 points (2 bytes per point) from the reference node. After locally computing Markov parameters, each node communicates 105 Markov parameters (each MP is 4 bytes); hence, a total of 6,300 bytes are transmitted. Again, assuming an effective data rate of 150 kbp, the wireless transceivers must remain active for 0.46 s. As a result, each transceiver consumes 27 mJ. Therefore, it can be concluded that each wireless sensor in the network preserves a total of 93 mJ by locally computing MPs and communicating the MPs instead of transmitting raw time-history data.

Conclusions

As wireless monitoring systems emerge as a viable alternative to traditional wired counterparts, scalable approaches to autonomously processing measurement data in the network are necessary. Embedded data processing has the benefit of improving system scalability, reducing demand on the wireless communication channel, and reducing the power consumption of the system battery-operated nodes. In this study, a decentralized approach to system identification was proposed for embedment within a wireless structural monitoring system. Specifically, extraction of nonparametric Markov parameters using input-output and output-only data locally stored at individual wireless sensor nodes allowed each node to convert its raw measurement data into a more compact representation prior to communication to a control server where ERA analysis was performed. The approach was scalable to large nodal densities because (1) the need for broadcasting data to the entire network was minimized (i.e., only the excitation or reference response time-history was broadcast) and (2) calculations (i.e., MP extraction) were performed in parallel independently by the pervasive wireless sensor nodes. By extracting 105 MP from 1,200-point response time-history records at 15 wireless sensor nodes, over 77% compression was accomplished. Although significant data compression was attained, system properties were still identified with a high-degree of accuracy.

For validation, a wireless monitoring system consisting of Narada nodes was installed on the mezzanine balcony of the Hill Auditorium. The wireless monitoring system was installed to control the excitation applied to the balcony, to sense the balcony response under the applied load, to communicate data, and to process measurement data in a scalable and autonomous manner. To validate the input-output MP extraction method embedded in-network, an electrodynamic shaker was also adopted. The MPs extracted in-network were found to be in complete agreement with MPs estimated off-line by a direct subspace identification method. The wireless monitoring system control server performed an ERA analysis using the MPs collected from the wireless sensor nodes, resulting in complete characterization of the system modal properties. The modal characteristics autonomously extracted by the wireless monitoring system using its in-network data processing were found to be within 2% of those extracted off-line by subspace identification for the first four modes.

Acknowledgments

The authors would like to gratefully acknowledge the generous support offered by the National Science Foundation under Grant CMMI-0726812 (Program Manager: Dr. S. C. Liu). Additional support was provided by the NIST Technology Innovation Program (Contract 70NANB9H9008). The authors would also like to thank Dr. Andrew Zimmerman, Mr. Kurt Thoma and Mr. Sean O'Connor (University of Michigan) for assistance during the experimental phase at Hill Auditorium.

References

Akaike, H. (1974). "Stochastic theory of minimal realization." *IEEE Trans. Autom. Control*, 19(6), 667–674.

Doebling, S. W., Farrar, C. R., and Prime, M. B. (1998). "Summary review of vibration-based damage identification methods." *Shock Vibr. Digest*, 30(2), 91–105.

Ewins, D. J. (2000). *Modal testing: Theory, practice and application*, Wiley, West Sussex, UK.

Ho, B. L., and Kalman, R. E. (1966). "Effective construction of linear state-variable models from input-output functions." *Regelungtechnik*, 14(12), 545–548.

Ibrahim, S. R. (1977). "Random decremental technique for modal identification of structures." *J. Spacecr. Rockets*, 14(11), 696–700.

Ibrahim, S. R., and Pappa, R. S. (1982). "Large modal survey testing using the Ibrahim time domain identification technique." *J. Spacecr. Rockets*, 19(5), 459–465.

James, G. H., and Carne, T. G. (1992). *Damping measurements on operating wind turbines using the natural excitation technique (Next)*, ASME, Houston, TX.

James, G. H., Carne, T. G., and Lauffer, J. P. (1995). "The natural excitation technique (next) for modal parameter extraction from operating structures." *Int. J. Anal. Exp. Modal Anal.*, 10(4), 260–277.

Juang, J. N. (1994). *Applied system identification*, Prentice Hall, Upper Saddle River, NJ.

Juang, J. N., and Pappa, R. S. (1985). "An eigensystem realization algorithm for modal parameter identification and model reduction." *J. Guid. Control*, 8(5), 620–627.

Juang, J. N., Phan, M., Horta, L. G., and Longman, R. W. (1991). "Identification of observer/Kalman filter Markov parameters." *Theory and Experiment*, NASA Langley Research Center, Hampton, VA.

Kim, J., Swartz, R. A., Lynch, J. P., Lee, J. J., and Lee, C. G. (2010). "Rapid-to-deploy reconfigurable wireless structural monitoring systems using extended-range wireless sensors." *Smart Struct. Syst.*, 6(5–6), 505–524.

Kung, S. (1978). "A new identification and model reduction algorithm via singular value decomposition." *12th Asilomar Conf. on Circuits, Systems and Computers*, Pacific Grove, CA.

Ljung, L. (1999). *System identification: Theory for the user*, Prentice Hall, Upper Saddle River, NJ.

Lynch, J. P., Sundararajan, A., Law, K. H., Kiremidjian, A. S., and Carryer, E. (2004). "Embedding damage detection algorithms in a wireless sensing unit for operational power efficiency." *Smart Mater. Struct.*, 13(4), 800–810.

Lynch, J. P., Sundararajan, A., Law, K. H., Kiremidjian, A. S., Kenny, T., and Carryer, E. (2003). "Embedment of structural monitoring algorithms in a wireless sensing unit." *Struct. Eng. Mech.*, 15(3), 285–297.

Lynch, J. P., Wang, Y., Loh, K., Yi, J. H., and Yun, C. B. (2006). "Performance monitoring of the geumdang bridge using a dense network of high-resolution wireless sensors." *Smart Mater. Struct.*, 15(6), 1561–1575.

Nagayama, T., and Spencer, B. F. (2007). "Structural health monitoring using smart sensors." *NSEL Report Series*, Univ. of IL at Urbana-Champaign, Urbana-Champaign, IL.

Peeters, B., and Roeck, G. D. (1999). "Reference-based stochastic subspace identification for output-only modal analysis." *Mech. Syst. Signal Process.*, 13(6), 855–878.

Peeters, B., and Ventura, C. E. (2003). "Comparative study of modal analysis techniques for bridge dynamic characteristics." *Mech. Syst. Signal Process.*, 17(5), 965–988.

Sim, S. H., Carbonell-Márquez, J. F., and Spencer, B. F. (2010). "Efficient decentralized data aggregation in wireless smart sensor networks." *Proc. of SPIE: Sensing and Smart Structures Technologies or Civil, Mechanical and Aerospace Systems*, SPIE, San Diego.

Straser, E., and Kiremidjian, A. S. (1998). *Modular, wireless damage monitoring system for structures*, John A. Blume Earthquake Engineering Center, Stanford, CA.

Swartz, R. A., Jung, D., Lynch, J. P., Wang, Y., Shi, D., and Flynn, M. P. (2005). "Design of a wireless sensor for scalable distributed in-network computation in a structural health monitoring system." *5th Int. Workshop on Structural Health Monitoring*, Palo Alto, CA.

Swartz, R. A., Lynch, J. P., Zerbst, S., Sweetman, B., and Rolfes, R. (2010a). "Structural monitoring of wind turbines using wireless sensor networks." *Smart Struct. Syst.*, 6(3), 183–196.

Swartz, R. A., Zimmerman, A. T., Lynch, J. P., Rosario, J., Brady, T., Salvino, L., and Law, K. H. (2010b). "Hybrid wireless hull monitoring system for naval combat vessels." *Struct. Infrastruct. Eng.*, 10.1080/15732479.2010.495398.

van Overschee, P., and de Moor, B. (1994). "N4sid: Subspace algorithms for the identification of combined deterministic-stochastic systems." *Automatica*, 30(1), 75–93.

van Overschee, P., and de Moor, B. (1996). *Subspace identification for linear systems*, Kluwer Academic, Dordrecht, Netherlands.

van Pelt, T. H., and Bernstein, D. S. (1998). "Least squares identification using μ-markov parameterizations." *37th IEEE Conf. on Decision and Control*, Tampa, FL.

Verhaegen, M. (1994). "Identification of the deterministic part of mimo state space models given in innovations form from input-output data." *Automatica*, 30(1), 61–74.

Viberg, M. (1995). "Subspace-based methods for the identification of linear time-invariant systems." *Automatica*, 31(12), 1835–1851.

Zimmerman, A. T., and Lynch, J. P. (2009). "A parallel simulated annealing architecture for model updating in wireless sensor networks." *IEEE Sens. J.*, 9(11), 1503–1510.

Zimmerman, A. T., Shiraishi, M., Swartz, R. A., and Lynch, J. P. (2008). "Automated modal parameter estimation by parallel processing within wireless monitoring systems." *J. Infrastruct. Syst.*, 14(1), 102–113.